

UC Irvine

UC Irvine Previously Published Works

Title

Reanalysis of primate brain circadian transcriptomics reveals connectivity-related oscillations

Permalink

<https://escholarship.org/uc/item/7mj396rz>

Journal

iScience, 26(10)

ISSN

2589-0042

Authors

Lee, Justine

Chen, Siwei

Monfared, Roudabeh Vakil

et al.

Publication Date

2023-10-01

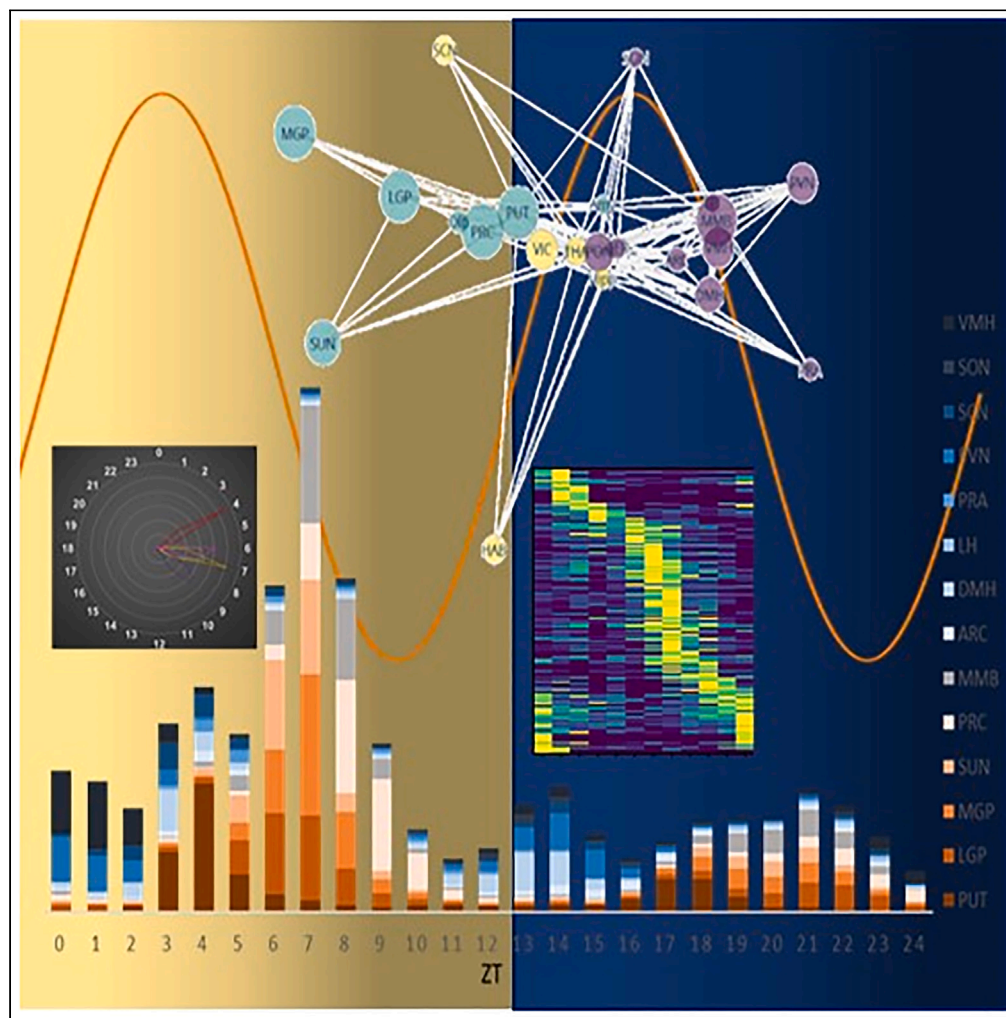
DOI

10.1016/j.isci.2023.107810

Peer reviewed

Article

Reanalysis of primate brain circadian transcriptomics reveals connectivity-related oscillations



Justine Lee, Siwei Chen, Roudabeh Vakil Monfared, ..., Kevin Beier, Pierre Baldi, Amal Alachkar

pfbaldi@uci.edu (P.B.)
aalachka@uci.edu (A.A.)

Highlights

Our study provides novel insights into circadian gene expression in neuronal circuits

Brain regions known for their circadian regulation show low robust transcript cycling

The mammillary body's gene oscillations challenge its traditional classifications

Some related brain regions share distinct gene expression patterns while others do not

Lee et al., iScience 26, 107810
October 20, 2023 © 2023 The Authors.
<https://doi.org/10.1016/j.isci.2023.107810>



Article

Reanalysis of primate brain circadian transcriptomics reveals connectivity-related oscillations

Justine Lee,^{1,9} Siwei Chen,^{2,9} Roudabeh Vakil Monfared,¹ Pieter Derdeyn,³ Kenneth Leong,¹ Tiffany Chang,¹ Kevin Beier,^{1,4,5,6,7} Pierre Baldi,^{2,7,8,*} and Amal Alachkar^{1,7,8,10,*}

SUMMARY

Research shows that brain circuits controlling vital physiological processes are closely linked with endogenous time-keeping systems. In this study, we aimed to examine oscillatory gene expression patterns of well-characterized neuronal circuits by reanalyzing publicly available transcriptomic data from a spatio-temporal gene expression atlas of a non-human primate. Unexpectedly, brain structures known for regulating circadian processes (e.g., hypothalamic nuclei) did not exhibit robust cycling expression. In contrast, basal ganglia nuclei, not typically associated with circadian physiology, displayed the most dynamic cycling behavior of its genes marked by sharp temporally defined expression peaks. Intriguingly, the mammillary bodies, considered hypothalamic nuclei, exhibited gene expression patterns resembling the basal ganglia, prompting reevaluation of their classification. Our results emphasize the potential for high throughput circadian gene expression analysis to deepen our understanding of the functional synchronization across brain structures that influence physiological processes and resulting complex behaviors.

INTRODUCTION

The brain, a remarkably complex organ, is organized into clusters of specialized structures responsible for regulating and performing specific functions. These structures interact and communicate with each other, forming interconnected networks known as neural assemblies or neuronal circuits.^{1,2} These circuits form the basis of various brain functions, including sensory processing, motor control, and higher-order cognitive functions.^{3–10} Neuronal circuits enable the harmonious functioning of both basic and higher-order brain activities, orchestrating a wide array of physiological processes and behaviors. Most physiological processes governed by neuronal circuits exhibit highly conserved circadian rhythms, suggesting synchronized activity and communication across nuclei within a particular circuit.^{11,12}

Circadian rhythms are endogenous biological oscillations with a periodicity of approximately 24 h that regulate diverse physiological processes and behaviors in living organisms. These brain circuits, which coordinate functional processes, play a significant role in the timing and rhythmic activity of various physiological functions like thermoregulation, food intake, and energy balance, to higher-order brain activities such as cognition, emotion regulation, and motor coordination.^{13–20}

The suprachiasmatic nucleus (SCN) in the hypothalamus serves as the central pacemaker or “master clock” of the mammalian circadian system.^{21–23} The SCN receives information relating to environmental cues, primarily light, and synchronizes endogenous circadian clock components to the 24-h light/dark cycle. By employing a variety of entrainment mechanisms, the SCN coordinates phase-setting of circadian rhythms in other brain regions, ensuring harmonious physiological functioning throughout the organism.²⁴ Beyond the SCN, other hypothalamic nuclei also exhibit timekeeping mechanisms and contribute to the regulation of circadian-sensitive physiological processes and behaviors, such as sleep/wake cycling and daily food intake.^{25–27} Moreover, rhythmic activity has been reported in multiple brain regions and structures, including the cortex, hippocampus, and amygdala, where neurons are believed to express all essential genes required for cell-autonomous circadian oscillations.^{20,28–33}

¹Department of Pharmaceutical Sciences, School of Pharmacy and Pharmaceutical Sciences, University of California, Irvine, Irvine, CA, USA

²Department of Computer Science, School of Information and Computer Sciences, University of California, Irvine, Irvine, CA, USA

³Mathematical, Computational, and Systems Biology Program, University of California, Irvine, Irvine, CA, USA

⁴Department of Physiology and Biophysics, School of medicine, University of California, Irvine, Irvine, CA, USA

⁵Department of Neurobiology and Behavior, University of California, Irvine, Irvine, CA 92697-4560, USA

⁶Department of Biomedical Engineering, University of California, Irvine, Irvine, CA 92697-4560, USA

⁷Center for the Neurobiology of Learning and Memory, University of California, Irvine, Irvine, CA 92697, USA

⁸Institute for Genomics and Bioinformatics, University of California, Irvine, Irvine, CA, USA

⁹These authors contributed equally

¹⁰Lead contact

*Correspondence: pfbaldi@uci.edu (P.B.), aalachka@uci.edu (A.A.)

<https://doi.org/10.1016/j.isci.2023.107810>



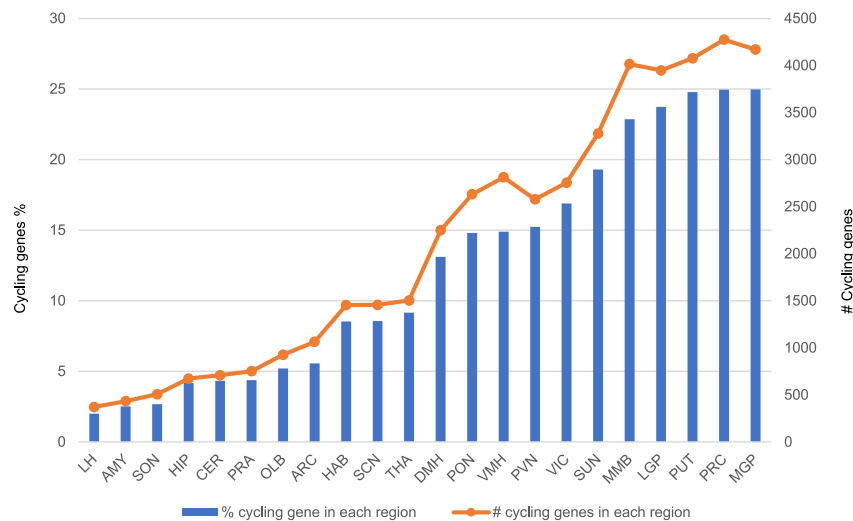


Figure 1. Abundance of circadian transcripts in the primates' brain regions

Histogram showing the number of cycling transcripts and their percentages of their total transcripts in 22 brain regions. AMY: amygdala, ARC: arcuate nucleus, CER: cerebellum, DMH: dorsomedial hypothalamus, HAB: habenula, HIP: hippocampus, PRC: prefrontal cortex, PUT: putamen, LGP: lateral globus pallidus, LH: lateral hypothalamus, MMB: mammillary body, MGP: medial globus pallidus, OLB: olfactory Bulb, PVN: paraventricular nucleus, PRA: preoptic area, PON: pons, SUN: substantia nigra, SCN: suprachiasmatic nucleus, SON: supraoptic nucleus, THA: thalamus, VMH: ventromedial hypothalamus, VIC: visual cortex.

We hypothesize that the genetic components within neuronal circuits display unique oscillating expression patterns, reflecting the synchronization of their respective molecular clocks through inter-neuronal communication. To investigate this hypothesis, we leveraged the largest available atlas of spatiotemporal gene expression in primates to analyze rhythmic transcriptomes across various brain regions. We then characterized gene expression patterns within selected circuits to better understand the relationship between circadian regulation and connectivity between anatomically defined brain regions.

Our findings reveal that gene expression cycling within brain regions traditionally associated with circadian regulation is less robust compared to regions not typically considered circadian in nature, and some anatomically or functionally related brain regions share distinct gene expression patterns while others do not. This observation provides novel insights into the encoding and execution of rhythmic behaviors and has implications for understanding the impact of circadian rhythm disruption on these processes.

RESULTS

Rhythmic gene expression across brain regions

Our comprehensive analysis identified 15,335 transcripts displaying circadian oscillation patterns in at least one brain region. Over 93% of these transcripts cycled with a periodicity of approximately 24 h, signifying circadian rhythmicity in their expression (Table S2). The prefrontal cortex (PRC) exhibited the highest number of circadian cycling transcripts (4,276), followed closely by the medial globus pallidus (MGP) (4,170) (Figure 1). Conversely, the lateral hypothalamus (LH) and amygdala (AMY) exhibited the lowest numbers, with 371 and 434 circadian transcripts, respectively.

It has been estimated that approximately 10% of genes in most tissues exhibit circadian expression.^{34,35} Based on this, the 22 brain regions were categorized into three groups: highly rhythmic, moderately rhythmic, and low rhythmic (Figure 1). Highly rhythmic regions had over 16% rhythmic transcripts, including the MGP, PRC, and putamen (PUT) (about 25% each), the lateral globus pallidus (LGP) and MMB (24% and 23%, respectively), substantia nigra (SUN) (19%), and visual cortex (VIC) (17%). Moderately rhythmic regions had 10–16% rhythmic transcripts, including the pons (PON), ventromedial hypothalamus (VMH), PVN (15% each) and dorsomedial hypothalamus (DMH) (13%). Low rhythmic regions had less than 10% rhythmic transcripts, including the olfactory bulb (OLB) (5%), arcuate nucleus (ARC) (6%), habenula (HAB), SCN, and thalamus (THA) (9% each). The LH, AMY, and supraoptic nucleus (SON) (2.5% each), and hippocampus (HIP), cerebellum (CER), and preoptic area (PRA) (4% each) had the lowest rhythmic transcripts (Figure 1).

Regional peaking times and temporal patterning in distinct neuronal circuits

Rhythmic transcripts exhibited region-specific expression peaks, reflecting the unique functional and anatomical characteristics of each brain region. We grouped brain regions by anatomical and functional proximity and then by when their transcript peaks occurred within one or more quarter-phase time intervals (Figures 2A, 2B, and S1). Brain structures like LGP, MGP, MMB, PON, PRC, PUT, SCN, SUN, and VMH showed over 50% of their rhythmic transcripts peaking within a narrow 6-h time interval or one quarter-phase (Figures 2A, 2B, and S1). These peak times coincided with the light phase of the 24-h cycle. The first quarter-phase (ZT0-ZT5) included PON, PUT, SCN, and VMH, while the

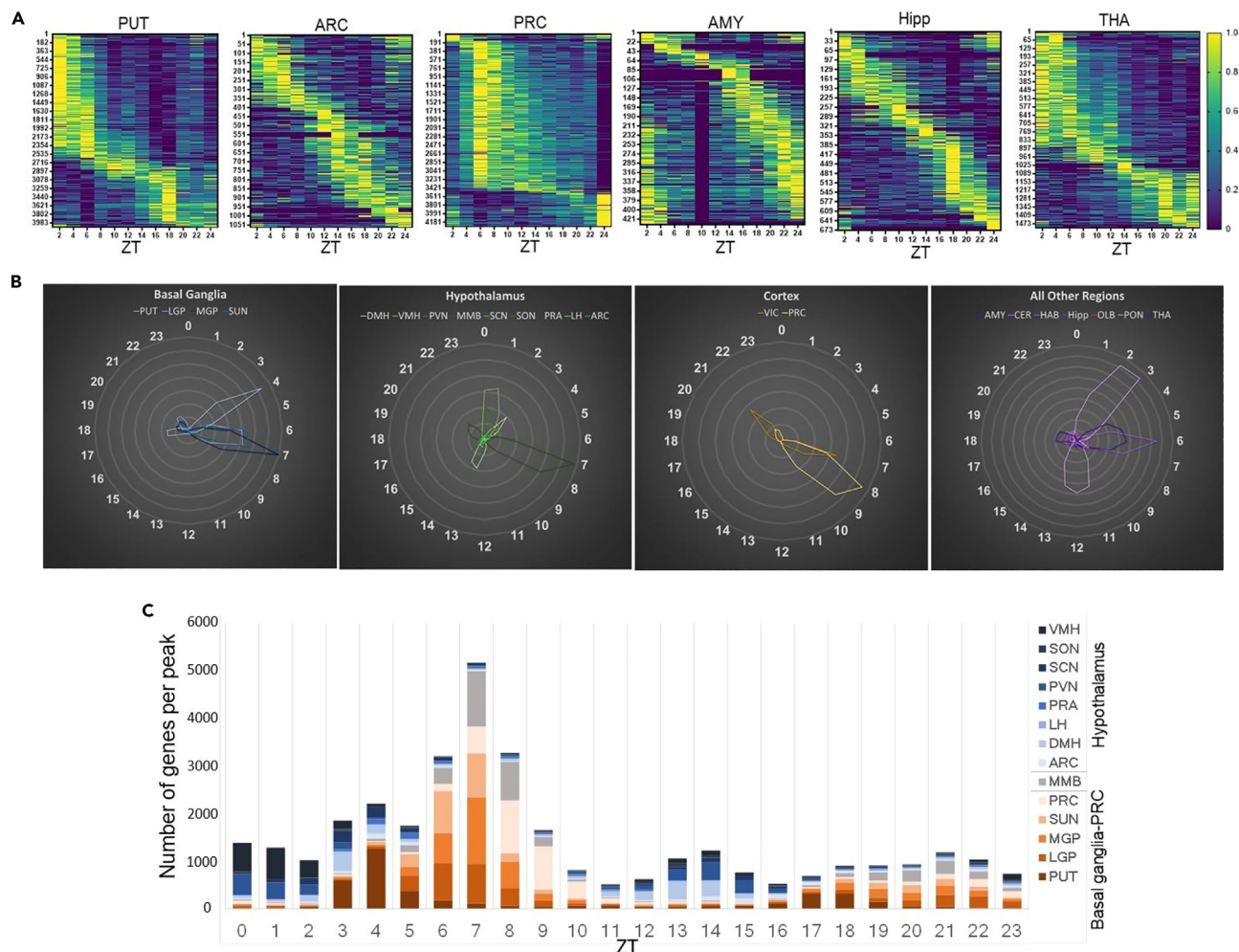


Figure 2. Brain circadian gene expression exhibit region-specific patterns

(A) Heatmap representation of 24-h oscillation of cycling genes in representative regions of the basal ganglia structures, hypothalamic nuclei, Cortices, and other brain regions with mean expressions normalized between 0 (blue) and 1 (yellow) and ordered by phase ($p < 0.05$), ZT: zeitgeber time.

(B) Radial diagram of the distribution of the peak phase of expression of the cycling genes in representative regions of the basal ganglia structures, hypothalamic nuclei, Cortices, and other brain regions. The radial plot displays phases (hr) on the circumference and the number of gene expression peaks on the radius.

(C) Cycling genes in brain regions mediating motor activity exhibit sharp expression peaks opposing to cycling genes of hypothalamic nuclei; Histogram showing number of cycling gene expression in the basal ganglia, hypothalamus, and PRC regions with the x axis corresponding to the hour of day, ZT: zeitgeber time.

second (ZT6-ZT11) had MMB, LGP, MGP, PRC, and SUN (Figures 2A, 2B, and S1). The DMH, PVN, and VIC showed peaks in two distinct quarter-phase intervals (Figures 2A, 2B, and S1). Regions like AMY, ARC, CER, LH, SON, HAB, HIP, OLB, PRA, and THA peaked in more than two intervals. Notably, PUT, MGP, and VIC had sharp peaks at specific times (Figures 2A, 2B, and S1).

Divergent temporal patterns in basal ganglia and hypothalamic circuits

Considering that the brain regions analyzed for cycling transcripts in the original study are part of distinct anatomical or functional circuits, we investigated the patterns of cycling transcripts in interacting nuclei. We determined inter-nuclei interactions based on relative anatomical position or functional connectivity and examined them for discernible patterns of overlapping cycling gene expression.

The basal ganglia (BG) circuit, which includes the PUT, LGP, MGP, and SUN has connections with THA and PRC, and is crucial for motor control, learning, and executive functions. High levels of cycling transcripts were seen in these regions (Figure 1), especially in PUT and MGP, the input and output regions of the BG, respectively. The rhythmic transcripts within the BG structures exhibited sharp peaking patterns, unfolding in a sequentially ordered manner from one region to the next. The PUT showed a strong circadian peak at ZT4 in the morning, whereas the SUN and LGP had similar peak timings, and together with MGP, followed PUT with sharp peaks 3–4 h later (ZT6-ZT7). Peak rhythmicity in the PRC occurred post-BG structures, around ZT8-ZT9 (Figures 2B and 2C).

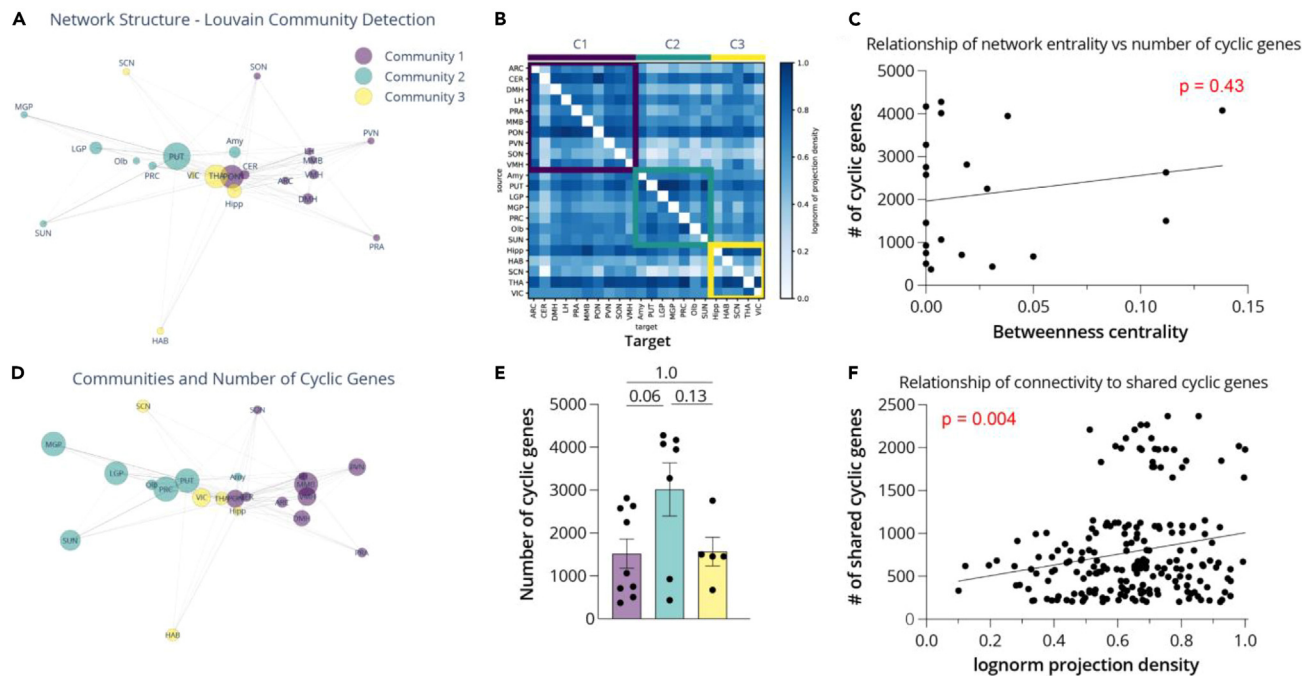


Figure 3. Relationship between cyclic gene expression and network connectivity

(A) Network connectivity matrix between the brain regions analyzed in this dataset. The Louvain Community Detection Algorithm was used to assign regions into Communities based on their connectivity patterns.

(B) Correlogram indicating the strength of input-output connections between all pairs of regions in the dataset. The color bar indicates the log-normalized projection density between any two regions.

(C) Linear regression plot of the relationship between the number of cyclic genes expressed in each region and the betweenness score of that region. No significant association was detected ($r^2 = 0.03$, $p = 0.43$).

(D) Visualization of the network connectivity matrix between the brain regions analyzed in this dataset, with the node size reflecting the number of cyclic genes expressed in that region.

(E) Bar graph of the number of cyclic genes in each region, binned by community. The number of cyclic genes was significantly different between these three communities (One-way ANOVA, $p = 0.05$), with regions in Community 2 expressing higher numbers of cyclic genes relative to Community 1 (t-test, $p = 0.06$) and Community 3 ($p = 0.13$). Communities 1 and 3 expressed similar numbers of cyclic genes ($p = 1.0$). T-tests include corrections for multiple comparisons.

(F) Linear regression plot of the relationship between the numbers of cyclic genes shared between two brain regions, and the log normalized projection density of the connection between them. A highly significant association was detected ($r^2 = 0.04$, $p = 0.004$). The pairs of brain regions with < 200 shared cyclic genes were excluded from this analysis.

In contrast to the circadian patterns observed in BG structures, the hypothalamic nuclei (ARC, DMH, LH, PRA, PVN, SCN, SON, and VMH) showed a more dispersed circadian transcript pattern, whereas MMB's pattern resembled that of BG structures more than hypothalamic nuclei (Figures 2B and 2C). Strikingly, peak times of cycling transcripts in the BG structures and hypothalamic nuclei were inversely related. The transcripts in BG structures reached their peak during the light phase, while those in the hypothalamic nuclei peaked during the dark phase (Figure 2C).

The number of cyclic genes in a brain region is related to its input and output connectivity patterns

We observed several interesting and surprising patterns in our data, including many of the brain regions that showed high levels of cyclic genes were in the BG circuit. However, brain connectivity is more complicated than classical models suggest, indicating that if we want to assess the relationship between connectivity and gene expression patterns, we need a quantitative, whole-brain mesoscale connectivity atlas. While this does not exist in primate species, the Allen Brain Institute provides an open access database of connectivity in the mouse brain.³⁶ By using this rodent atlas, we could approximate the strength of connections between brain regions. While connectivity in the rodent brain is certainly different than connectivity in the primate brain, many key brain structures are conserved between the species, allowing us to use this as a first-order approximation of the relationship between cyclic gene expression and connectivity.

We first built a model network between the brain regions we are examining in this study. Using the Louvain Community Detection algorithm, we detected three communities of brain regions (Figure 3A). The Louvain algorithm identifies communities—groupings of nodes that maximize modularity such that nodes within community preferentially connect with each other over those outside of their community. The

PUT, THA, and PON were the most extensively interconnected of these regions, as indicated by their high betweenness centrality score (Figure 3A). We also created a correlogram to detail the quantitative relationship between input/output connectivity for each pair of brain regions (Figure 3B). As expected, regions in the BG cluster into a common community (Community 2), while most hypothalamic regions cluster into Community 1. Community 3 contains mostly thalamic, epithalamic (HAB), and hippocampal regions, with the exception of the SCN; this is likely because the SCN receives strong innervation from the lateral geniculate nucleus (LGN) of the thalamus, pulling it into a community with THA and not hypothalamic regions.

Based on this connectivity matrix, we first wanted to explore whether the number of connections each brain region received was related to the number of cyclic genes that the region expressed. We did not find a significant correlation between these metrics ($p = 0.43$; standard error of slope = 7,397, Y-intercept = 355; Figure 3C), indicating that whether or not a region serves as a hub gene has no effect on the number of cyclic genes it expresses. Next, we aimed to explore the relationship between the innerconnectivity of any two regions and the numbers of cyclic genes that are shared between these regions. We first visualized the connectivity network, using the same edges as in Figure 3A, and visualized each node by correlating the size with the total number of cyclic genes expressed in that brain region (Figure 3D). Using this approach, we find that brain regions in Community 2, which contains regions in the BG, have higher levels of cyclic genes than regions in Communities 1 or 3 (Figure 3D). We quantified the number of cyclic genes in each region within each community, and found a strong trend toward a significant difference between groups (One-way ANOVA, $p = 0.053$; Figure 3E). We followed up on this finding by building a mixed effects model, modeling community membership as a random effect on number of cyclic genes. Community membership accounted for 26% of variance in number of cyclic genes due to random effects, suggesting community membership is related to the number of cyclic genes expressed in a given brain region. Notably, we excluded the MMB from the previous analysis, given that its cyclic gene expression pattern more closely aligns with patterns observed in BG structures (as described later in this manuscript).

Lastly, to more quantitatively explore the relationship between the number of shared cyclic genes and the strength of projection between them, we performed a linear regression analysis of the numbers of shared cyclic genes between pairs of regions relative to the log-normalized projection density between them (Figure 3F). Region pairs with 200 or fewer shared cyclic genes were discarded as they were overrepresented in our data. We found a statistically significant correlation, indicating that the number of shared cyclic genes between two regions is strongly related to how directly interconnected those two regions are ($p = 0.004$; standard error of slope = 214.5, Y-intercept = 143). Data failed a test for heteroscedasticity using the Breusch-Pagan test ($p = 0.006$), so we tested the linear coefficient p value for bias by performing scrambled linear regression tests. We scrambled the relationship of number of shared genes with the projection strength and performed a linear regression test 1000 times and recorded all the linear coefficient p values. The p value for the actual data were less than 99.5 percent of all scrambled p values, suggesting that it is still statistically significant. Even so, we also tested these data for monotonicity with a Spearman correlation test, and found a positive relationship between them ($p = 0.022$), providing further evidence of a relationship between connectivity and the number of shared cyclic genes between brain sites.

Overlapping expression of circadian transcripts across brain regions

We found varying overlaps in circadian transcript expression across brain regions, with two (Metazoa_SRP and U6) shared globally (Table S3). Half the regions shared 106 transcripts, while 5220 transcripts were unique to individual regions.

There were 231 regional overlaps of the circadian transcriptome, with the number of overlapping transcripts ranging from 15 (between AMY and LH) to 2368 transcripts (between LGP and MGP, Figure 4A). MGP had the highest number of cyclic transcripts overlapping with other regions (3969). Besides the MGP, the LGP, SUN, MMB, PRC, PUT, and SCN shared over 90% of their cycling transcripts (Figure 4B). The LH had the least overlap (259 transcripts, 70% interregional) (Figure 4B). Most regions showed the greatest number of cyclic transcript overlaps with the MGP, PRC, LGP, and MMB (Figure S2). BG structures exhibited a higher overlap of circadian transcripts among each other than with other brain regions, with each nucleus sharing at least 45% of their cycling transcripts with the others (Figures 5A and S2; Table S3). They shared 1083 circadian transcripts among themselves, and 871 with the PRC (Figures 5A and S2; Table S3). These shared transcripts showed sharp peaks at specific times: 4ZT for PUT, 6–7ZT for SUN and LGP, 7ZT for MGP, and 8–9ZT for PRC (Figure 5B). Interestingly, the order of these peaks aligned with the sequence of anatomical connectivity in controlling movement.

Circadian transcripts in hypothalamic structures showed minimal overlap with each other and other brain regions (Figure S3). Given the low degree of interregional overlap across hypothalamic structures (excluding the MMB), we analyzed shared transcripts across different hypothalamic nuclei, assuming that hypothalamic circuits encompassed at least three nuclei. This analysis produced 84 sets of three hypothalamic nuclei (Table S3). The overlap of circadian transcripts across these sets ranged from five transcripts (in ARC/LH/SON and MMB/LH/SON sets) to 348 transcripts (in DMH/MMB/PVN set) (Table S3).

Though traditionally classified as a hypothalamic nucleus due to its location, MMB displayed greater gene overlap with BG structures (PUT, LGP, MGP, and SUN) than other hypothalamic nuclei (Figures 5C and S3). Over 1000 circadian transcripts were shared between MMB and any two BG structures, contrasting with only 106–348 shared with any two hypothalamic nuclei (Figures 5C and S3). Shared circadian genes across MMB and BG showed a pronounced peak at 4ZT for PUT and at 7ZT for LGP, MGP, and MMB (Figure 5D).

Finally, clock genes (Dbp, Per1, Per2, Per3, Cry1, Cry2, Clock, Bmal1, Bmal2, Npas2, Ror2, Nr1d1, and Nr1d2) exhibited circadian rhythms in at least one BG and hypothalamic structures, except the LH (Figure 5E). Notably, the BG structures PUT and MGP expressed the highest number of circadian clock genes (seven), whereas the hypothalamic MMB expressed the most circadian clock genes (eight) (Figure 5E).

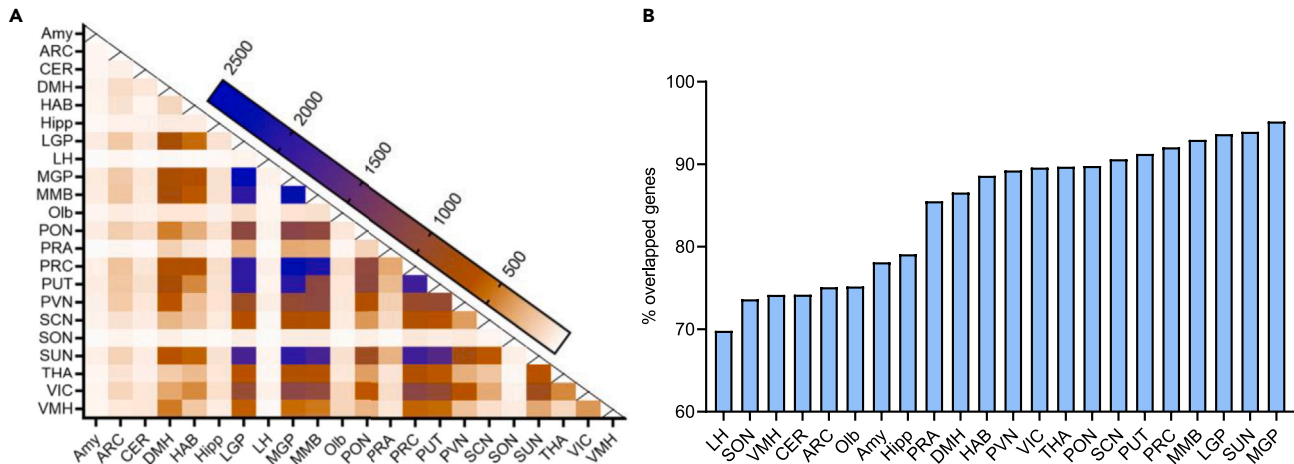


Figure 4. Overlapping expression of circadian transcripts across brain regions

(A) Heatmap of region-by-region overlap showing overlapping expression of every region's circadian transcriptome with all other brain regions contributing a total of 231 regional overlaps.

(B) Percentage (y axis) of overlapped genes in each brain region (x axis). MGP showed highest rate of overlapping circadian genes with other regions (95% of its circadian gene) while LH showed the lowest overlapping of cycling genes with other regions (<70% of its circadian genes).

Pathway enrichment analysis of cycling transcripts

We performed a pathway enrichment analysis on cycling transcripts in each brain region, calculating a Log₂ fold enrichment (Log₂(FE), with a cut-off of a false discovery rate (FDR) < 0.05. Brain regions displaying a Log₂(FE) greater than 3 are presented in Figure 6A, and the rest are presented in Figure S3. We classified brain regions by the density of associated pathways into low, moderate, or highly enriched groups, based on the number of enriched pathways. Low enrichment regions were AMY (enriched in transmembrane receptor protein tyrosine kinase signaling pathway and circadian rhythm), LH (neuropeptide signaling pathway), OLB (extracellular matrix organization), PRA (cell communication regulation), SCN (posttranslational gene expression regulation), and SUN (base excision repair) (Figures 6A and S4). Moderate enrichment pathways' numbers were seen in ARC, DMH, MMB, PON, PVN, and THA, whereas HAB, LGP, MGP, PRC, PUT, SON, VIC, and VMH exhibited numerous enrichment pathways (Figures 6A and S4). Notably, HIP and CER showed no pathway enrichment, and the number of cycling transcripts in certain regions did not correlate with enriched pathways.

Circadian rhythm and related processes were enriched pathways in cycling transcripts of many regions, particularly the AMY, MMB, HAB, PRC, SON, THA, VIC, and VMH. Pathways regulating proteasomal ubiquitin-dependent protein processes were enriched in cycling transcripts of the DMH, LGP, MGP, PRC, PUT, PVN, SUN, VIC, and VMH. Microtubule-based process pathways were enriched in the ARC, DMH, MGP, PRC, PVN, and VIC. Specifically, regulatory pathways involving microtubule-based organelles, such as cilia and centrosomes, were enriched in the ARC and DMH, respectively (Figures 6A and S4).

Pathways linked to RNA splicing and post-transcriptional regulation were enriched in the HAB, PON, SCN, THA, VMH, and VIC. Mitochondrial processes were significant in MMB, PUT, PON, VMH, and VIC. MGP, HAB, and PRC showed enrichment in axonal myelination pathways, whereas LGP, PUT, and VIC favored the ERAD (endoplasmic reticulum to Golgi vesicle-mediated transport) pathway. Lipid response and metabolism pathways were enriched in MGP, DMH, HAB, PRC, PVN, and MMB, whereas DNA transcription and damage response pathways were enriched in DMH, HAB, MGP, MMB, LGP, PON, PVN, PUT, and VIC. Telomere maintenance pathways were active in LGP, PON, and VMH, while HAB, PON, VMH, and MGP were enriched in histone modification pathways. Synapse development pathways were enriched in SON and VMH, with SON, VMH, and PRC. The regulatory pathway of calcium-dependent exocytosis was enriched for the PRC, PVN, and AMY, and protein localization to the nucleus was enriched for the LGP and PUT. Response to insulin and regulation of cell glucose pathways were enriched for the HAB and VMH. The neurogenesis pathway was enriched for the SON, HAB, and PRC, and the WNT pathway was enriched for the LGP and PUT (Figures 6B and 6C).

We conducted a gene analysis across 15 brain regions, representing two-third (68%) of all areas studied. The results revealed shared biological pathways related to circadian rhythm, positive triglyceride biosynthesis regulation, negative peptidyl-threonine phosphorylation regulation, ncRNA transcription regulation, base-excision repair, histone deacetylation, and JUN kinase activity regulation (Figure 6B).

Shared cycling genes across the BG structures showed enrichment in pathways for positive cholesterol efflux regulation, chondroitin sulfate proteoglycan metabolism, selective autophagy, snRNA metabolism, endoplasmic reticulum stress response regulation, fatty acid catabolism, NADH dehydrogenase complex assembly, mitochondrial respiratory chain complex I assembly, and positive regulation of proteasomal ubiquitin-dependent protein catabolism (Figure 6C). For hypothalamic circuits, we analyzed shared transcripts across 84 sets of three hypothalamic nuclei. This analysis, however, did not reveal any significantly enriched pathways.

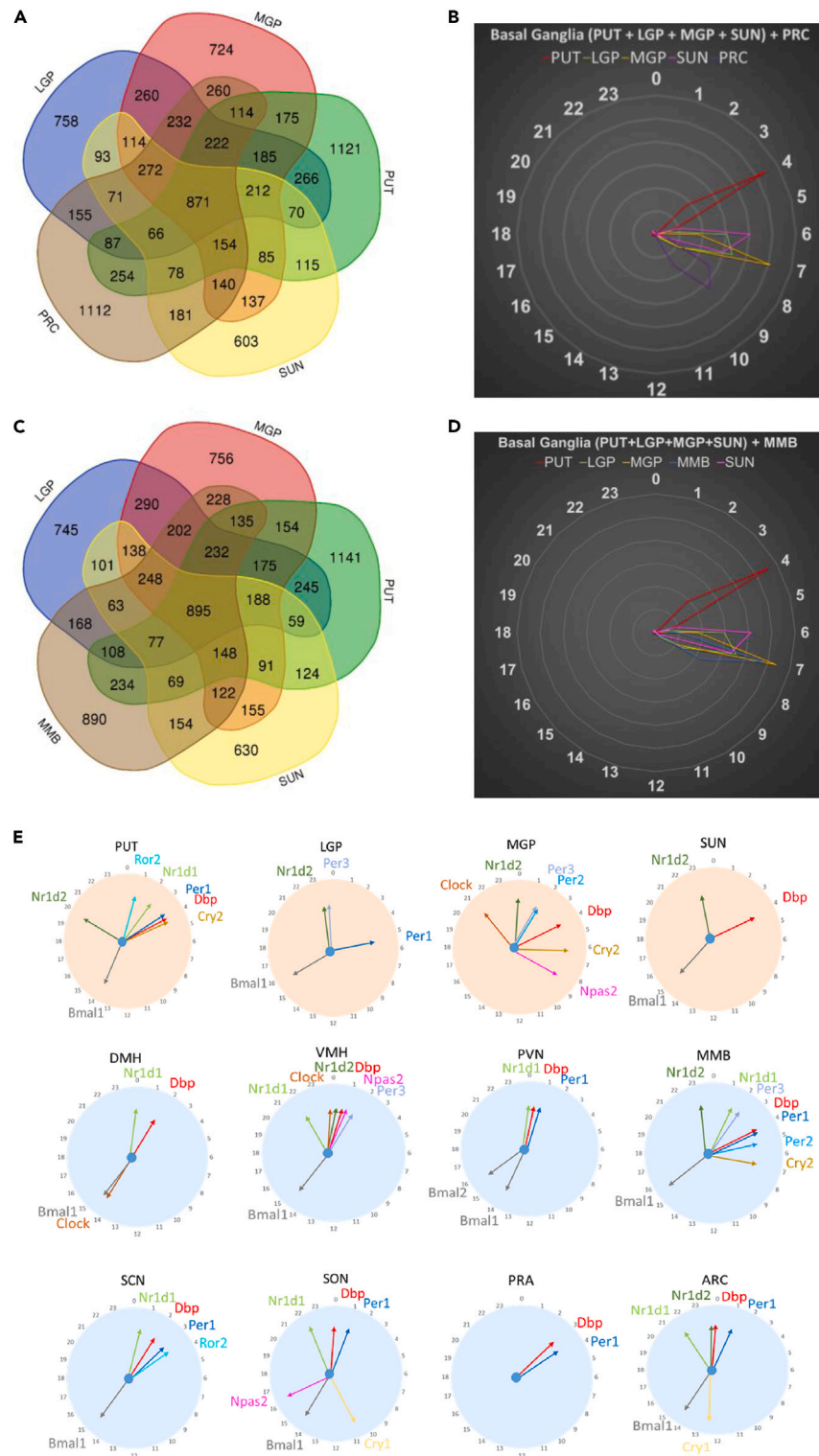


Figure 5. Rhythmic patterns of the shared cycling transcripts in the basal ganglia-cortex and hypothalamic circuits

(A) Venn diagram showing the shared cyclic transcripts across the structures of the basal ganglia circuit and prefrontal cortex.

(B) Radial plot of the peak phase of expression of the shared circadian genes across the structures of the basal ganglia and the prefrontal cortex.

(C) Venn diagram showing the overlap of regions of the basal ganglia structure with MMB.

(D) Radial plot of the distribution of the peak phase expression of shared circadian genes in the basal ganglia and MMB.

(E) Radial plot showing peak expression phase of the clock genes with circadian pattern in basal ganglia and hypothalamic structures.

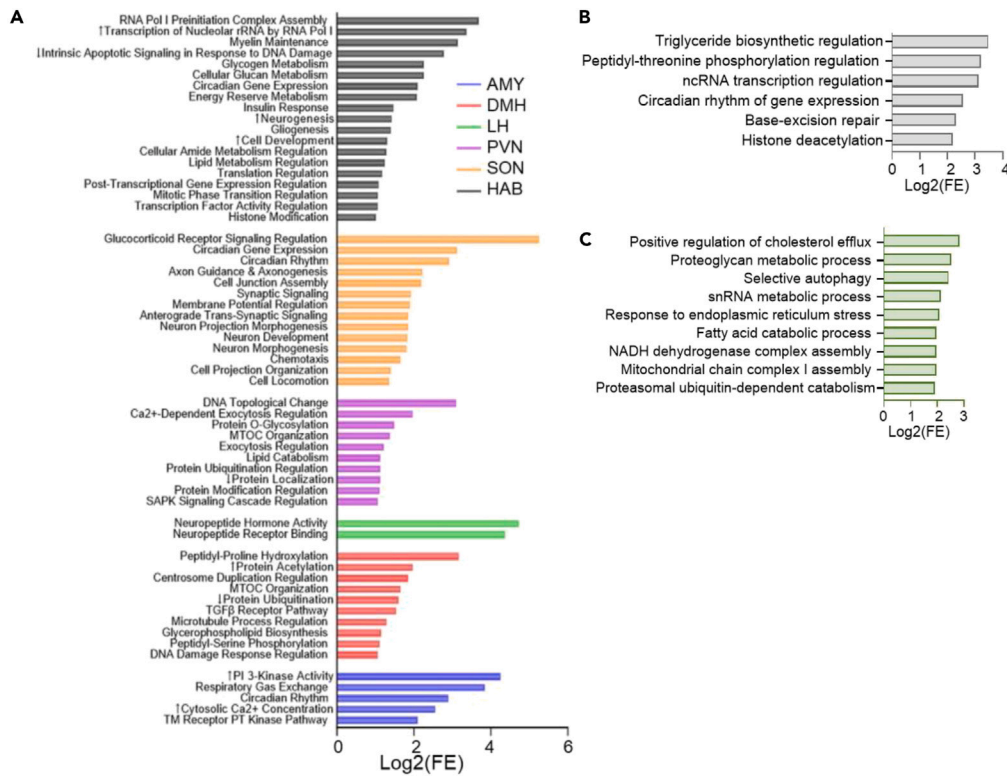


Figure 6. Enrichment of the biological pathways of cycling transcripts in different brain regions

(A) Enriched pathways in different brain regions displaying a $\text{Log}_2(\text{FE})$ greater than 3.

(B) Enriched pathways in shared circadian transcripts across two-third (15) brain regions and (right) 50% of all the brain regions (11 regions).

(C) Enrichment pathways in shared circadian transcripts in the basal ganglia.

DISCUSSION

In this study, we investigated whether genetic components of neuronal circuits display distinct oscillating expression patterns based on synchronized molecular clocks in interneuronal communication. We also tested if brain regions with more rhythmic physiological functions express more circadian genes than those traditionally less linked with circadian function. We analyzed publicly available transcriptomic data from a non-human primate's spatiotemporal gene expression atlas. Unexpectedly, we found that nuclei involved in rhythmic processes show moderate to low transcript rhythmicity, and some anatomically or functionally related brain regions share distinct gene expression patterns while others do not.

Methodological consideration

While numerous studies have analyzed oscillatory expression patterns in peripheral tissues of humans and animals, including primates and rodents, only a few have focused specifically on brain regions and assessed the data derived from the underlying circuits. The dataset used here encompassed an atlas of transcriptomic data from 64 tissues, a third of which were brain regions.³⁴ Our analysis revealed significant differences in the number of circadian transcripts identified by BIO_CYCLE, used in our study, compared to MetaCycle, used in the original study. Except for the paraventricular nucleus (PVN), BIO_CYCLE identified more circadian transcripts in all brain regions than MetaCycle.³⁷ BIO_CYCLE, being a Bayesian algorithm, provides a statistically robust framework for detecting cyclical patterns in time-series data. Its in-built features, including the ability to handle missing data, the use of phase-adjusted errors, and the assessment of periodicity across multiple cycles, make it particularly suitable for our analysis. Furthermore, BIO_CYCLE's Bayesian framework enables more effective handling of uncertainty, which is beneficial in the context of high-throughput transcriptomic data, where intrinsic variability is common.^{38–42}

As noted in the results section, we used a mouse mesoscale brain atlas to model connectivity, and related this to the cyclic gene expression patterns observed in the primate brain. Of course, the brain-wide connectivity patterns between rodents and primates are not wholly conserved. In addition, the mouse is a nocturnal species, while the baboon is diurnal; there is thus some possibility that the relationships between cyclic gene expression and anatomical connectivity may differ between the two species. Thus, a degree of caution should be taken in directly extrapolating these results directly into the relationship between cyclic gene expression and connectivity in baboons. Nonetheless, despite these key differences in animal behavior, the interconnectivity between key brain structures such as the BG is largely conserved across species. This certainly is the case between those evolutionally relatively closely related, such as the mouse and primate, but also in species that

are less closely related, such as mice and birds and reptiles.^{43–45} In all, the results relating connectivity to cyclic gene expression are best viewed as a first-order approximation of the relationship between these factors, rather than a rigorous quantitative assessment. Nonetheless, we believe that the key finding of these analyses—that the number of shared cyclic genes between two brain regions is related to the interconnectivity between them—is supported by the evidence presented in our manuscript. This finding also is intuitively logical, and suggests that brain regions that function within a network have similar shared transcripts, and suggests that the cyclic nature of these genes extends beyond one brain region, but likely impacts the functional output of entire circuits. How entire circuits may be impacted by the shared cyclic nature of these genes, however, remains to be explored.

Brain structures typically associated with regulating circadian processes do not display robust cycling patterns in their gene expression

It is reasonable to presume that brain structures mediating more rhythmic functions, such as hypothalamic nuclei, hippocampus, and amygdala, would express more circadian genes. This presumption, indeed, influenced prior research, evident in the original transcriptomic atlas focusing on circadian genes from nine hypothalamic subregions, whereas other regions, such as the striatum with its distinct nuclei, were underrepresented or neglected, focusing only on the putamen. Vital structures like the ventral tegmental area and SUN pars reticulata (a subdivision of the SUN) were also omitted.³⁴

Contrary to expectations, our analysis revealed that hypothalamic nuclei, which govern various rhythmic physiological processes, exhibited only moderate to low gene rhythmicity, with the MMB as an exception.^{28,46} Notably, the LH, a key player in circadian functions, displayed the lowest rhythmicity. Our enrichment analysis revealed a limited number of defined circadian pathways, although the enriched pathways did involve neuropeptides associated with circadian functions like feeding behavior and sleep. Similar to the LH and other hypothalamic structures, the HIP, known for its circadian activity and synaptic plasticity modulation,^{47–52} also showed very low levels of rhythmic transcripts. Our findings revealed that the PRC, MMB, and BG nuclei (PUT, LGP, MGP, and SUN) have the highest number of circadian genes, a surprising result given the traditional association of BG nuclei with motor control, learning, and executive functions rather than circadian systems. The underexplored MGP, showing the highest proportion of cycling transcripts across all brain regions, and LGP present an unexpected aspect of rhythmic process, aligning with recent findings of a high proportion of circadian genes in human PUT.^{53–55} Remarkably, the peak times of cycling transcripts in the BG structures and hypothalamic nuclei were inversely related. The cyclic transcripts in BG structures reached their peak during the light phase, while those in the hypothalamic nuclei peaked during the dark phase. This contrasting expression is interesting in light of the distinct functional roles of the BG in motor functions and hypothalamic circuits in sleep.

The MMB, currently classified as a hypothalamic structure, demonstrated high rhythmicity akin to the BG nuclei and PRC rather than its hypothalamic counterparts. Given MMB's involvement in memory and movement control and its strong gene cycling correlation with BG, we suggest reconsidering its categorization. This could also have implications for disorders like Wernicke-Korsakoff syndrome, affecting the MMB, as it could enhance our understanding of motor-related aspects and refine treatment strategies.^{56,57}

Pathway enrichment analysis of cyclic transcripts reveals discrete roles of different brain structures

Our pathway enrichment analysis of cycling transcripts demonstrated distinct roles of various brain structures. Notably, proteasomal ubiquitin-dependent protein degradation pathways were enriched in 9 out of 22 brain regions. These pathways are responsible for breaking down proteins and recycling amino acids to create new proteins. Given that organisms require diverse proteins for time-dependent and region-specific functions and protein degradation rates fluctuate widely, robust cycling behavior in gene expression for these pathways is anticipated to match daily cellular activity variations.^{58–65} The malfunction of this pathway due to deficient Ubiquitin ligase (Ubl) expression has been linked to disrupted circadian systems and impaired neuropeptide transport in animal Ubl knockout models.^{58,60,62–65} Microtubule-based processes, facilitating intracellular protein transport, were found enriched in most of the same brain regions as this protein regulatory pathway.⁵⁹ Additionally, an overlap was observed between areas where ERAD, a vesicle-mediated transport pathway, and Ub regulatory pathways were enriched (i.e., LGP, PUT, and VIC). This implies a deeper functional interrelationship among these pathways, contributing to similar pathway enrichments across multiple brain regions.

Despite its role in circadian-sensitive memory processes, our analysis found that the HIP did not show pathway enrichment for any cycling gene. The HIP clock, governed by the transcription factor BMAL1, influences time-dependent memory deficits, and reduced BMAL1 levels impact neurogenesis in the HIP.^{66–68} It is plausible that the HIP function could be indirectly affected by the cyclical gene expression patterns in other areas, like the HAB, a region interconnecting the BG and the limbic system, thereby influencing the limbic memory circuit that relies on the HIP.⁶⁹

Functional and anatomical circuit-driven transcriptomic circadian rhythm

We sought to determine whether cycling genes in anatomically and functionally defined brain circuits, such as the BG and hypothalamic structures, exhibit coordinated oscillatory patterns. These patterns could shed light on the information flow within neuronal circuits, giving rise to complex behaviors.

Circadian oscillator network within the hypothalamus

The hypothalamus, composed of interconnected nuclei, and housing central “master” clock in the SCN, acts as a network of oscillators controlling numerous physiological and behavioral aspects. Circadian clocks, which are sensitive to temperature changes, integrate cues such as

body temperature fluctuations, informing thermoregulatory mechanisms. This coordinated activity between SCN and other nuclei is vital for rhythmic temperature control. Moreover, SCN-independent hypothalamic clocks help synchronize diurnal energy expenditure and thermogenesis.^{70,71}

Key thermogenic circuits involve the ARC, PRA, DMH, and LH, which help regulate body temperature and metabolism.⁷² The thermoregulatory processes impact metabolic activities like energy expenditure and adaptive thermogenesis, which responds to environmental changes like temperature fluctuations and food intake. Studies have shown body temperature fluctuations coincide with metabolic heat production in constant darkness and temperature-controlled environments.⁷³ Energy homeostasis, achieved by balancing energy expenditure with food intake, involves hypothalamic nuclei like the ARC, DMH, PVN, and LH, which cooperate with the SCN to generate feeding rhythms.^{74–78} Neural networks connecting these hypothalamic nuclei express signaling molecules affecting appetite, such as proopiomelanocortin (POMC), neuropeptide Y (NPY), and agouti-related peptide (AgRP).⁷⁹ The sleep/wake cycle, another circadian-related behavior, is controlled by neural connections from the DMH and LH to the PRA.^{80–82} The DMH, receiving direct input from the SCN, is instrumental in maintaining the sleep/wake cycle's circadian rhythm.^{83,84} Its neuronal projections to the POA and LH support rhythmic changes, enabling transitions between wakefulness and sleep.⁸⁴ Despite the known interactions among hypothalamic nuclei, our findings surprisingly reveal no significant overlap among cyclic transcripts or any metabolic or functional pathways across these nuclei. This may suggest more parallel than hierarchical or synchronized action. We recognize that our analysis of bulk RNAseq data have a significant limitation regarding its ability to reflect the cellular heterogeneity within each brain nucleus. Notably, structures such as the hypothalamic nuclei are comprised diverse neuronal populations, each of which could exhibit distinct rhythmic gene expression patterns. This complexity might be masked when analyzing bulk tissue transcriptomic data, potentially leading to an underrepresentation or overlook of individual population-specific rhythmicities. This potential confounder is particularly relevant when considering that distinct neuronal populations within the same nucleus might have gene expression peaks at varying times of the day. Such complexities could result in an apparent lack of rhythmicity at the tissue level, even as a variety of rhythmic patterns occur at the cellular level.

Circadian oscillator network within the basal ganglia circuit

The BG circuit, comprising the PUT, MGP, LGP, and SUN, controls movement, learning, executive functions, and emotional processing. Our study identified rhythmic dopamine D2 receptor expression in the PUT, with most rhythmic genes in the BG nuclei clustering in one or two narrow time windows. The order of peak times for shared rhythmic genes was PUT > SUN > LGP/MGP, occurring within 1–2 h. However, the precise nature of these circadian oscillations is unclear due to the uncertainty regarding SUN tissues analyzed, which could involve dopaminergic (SUNc) or GABAergic (SUNr) neurons. The sequential peak times might be linked to changes in locomotor activity, given the variation in activity levels and molecular factors across BG nuclei. During rest periods, striatal neurons are generally inactive, with information processing and relay occurring during movement initiation.^{85,86} The complex architecture of BG circuitry might underpin the sequential peak times, with structures coordinating their activities after periods of sleep-related inactivity. While locomotor activity exhibits circadian rhythms, traditional views do not consider BG structures involved in motor activity as part of the circadian system. Nonetheless, our findings indicate high circadian transcript numbers in these regions, possibly due to motor activity suppression during sleep and the need for rapid activation upon waking.

Sensory decoupling and sleep-related muscle relaxation prevent execution of motor plans in response to external or internal triggers.⁸⁷ It is plausible that circadian rhythm may influence mechanisms underlying these processes, with genes showing oscillating expression patterns in relevant brain regions corresponding to sleep/wake cycling. Moreover, BG neurons' spatiotemporal expression of rhythmic genes follows sequential order of functional circuitry controlling movement. Our findings suggest that drugs targeting BG circuits (e.g., via D2 receptors) may be influenced by rhythmic cycling. As BG abnormalities are implicated in schizophrenia, Tourette syndrome, Parkinson's disease, and obsessive-compulsive disorder, our results may have clinical implications for therapeutic administration timing. Further research on circadian rhythmicity and pharmacotherapeutics' dosing schedules could enhance medication efficacy by leveraging natural cycling of circadian processes.

Concluding remarks

Our investigation into spatiotemporal gene expression patterns in brain regions with related anatomical and functional properties has revealed interesting insights into circadian processes. We found that brain structures traditionally associated with circadian functions, like hypothalamic nuclei, do not always exhibit strong gene cycling. Conversely, regions like the BG, not typically linked to circadian physiology, display dynamic cycling patterns. The MMB, often considered hypothalamic nuclei, exhibited gene oscillations similar to BG nuclei, potentially impacting their classification. Further investigation into the interregional effects of pathway activation could enhance our understanding of molecular activity's correlation with circuit functions of different brain structures.

Limitations of the study

We recognize the limitations of our study associated with using publicly available data and the intrinsic limitations tied to transcriptomic analysis. The extrapolation of findings from a non-human primate model to human physiology should be done with caution. Our focus on brain structures excludes potential connections with key peripheral organs such as the liver, suggesting an avenue for future research. Additionally, our largely computational approach lacks experimental validation from model organisms, restricting the establishment of causal relationships between gene oscillations and their roles across brain regions. Despite these caveats, our work is expected to provide a solid foundation for future studies exploring the complexities of circadian rhythms.

STAR★METHODS

Detailed methods are provided in the online version of this paper and include the following:

- **KEY RESOURCES TABLE**
- **RESOURCE AVAILABILITY**
 - Lead contact
 - Materials availability
 - Data and code availability
- **METHOD DETAILS**
 - Transcriptomic data
 - Circadian analysis
 - Network Construction
 - Network statistical analysis
 - Functional enrichment analysis
 - Statistical analysis

SUPPLEMENTAL INFORMATION

Supplemental information can be found online at <https://doi.org/10.1016/j.isci.2023.107810>.

ACKNOWLEDGMENTS

The work of SC and PB was supported in part by NIH grant GM123558. The work of AA was supported in part by R01-HL147311-02S1. PD was supported by NSF GRFP DGE-1839285, and KTB was supported by NIH DP2-AG067666, R01-NS130044, R01-DA056599R01-DA054374, TRDRP T31KT1437 and T31IP1426, One Mind OM-5596678, Alzheimer's Association AARG-NTF-20-685694, New Vision Research CCAD2020-002, and BrightFocus A2022031S.

AUTHOR CONTRIBUTIONS

Conceptualization, A.A., P.B., K.B.; Methodology, S.C., P.B.; Investigation, S.C., R.V.M., P.D., K.L.; Writing – Original Draft, J.L., T.C., A.A.; Writing – Review & Editing, J.L., T.C., K.B., A.A.; Funding Acquisition, A.A., P.B.; Supervision, A.A., P.B., K.B.

DECLARATION OF INTERESTS

The authors declare no competing interests.

Received: May 8, 2023

Revised: July 22, 2023

Accepted: August 30, 2023

Published: September 1, 2023

REFERENCES

1. Kelley, D.B., Ballagh, I.H., Barkan, C.L., Bendesky, A., Elliott, T.M., Evans, B.J., Hall, I.C., Kwon, Y.M., Kwong-Brown, U., Leininger, E.C., et al. (2020). Generation, Coordination, and Evolution of Neural Circuits for Vocal Communication. *J. Neurosci.* *40*, 22–36. <https://doi.org/10.1523/JNEUROSCI.0736-19.2019>.
2. Lerner, T.N., Ye, L., and Deisseroth, K. (2016). Communication in Neural Circuits: Tools, Opportunities, and Challenges. *Cell* *164*, 1136–1150. <https://doi.org/10.1016/j.cell.2016.02.027>.
3. Aristieta, A., and Gittis, A. (2021). Distinct globus pallidus circuits regulate motor and cognitive functions. *Trends Neurosci.* *44*, 597–599. <https://doi.org/10.1016/j.tins.2021.06.001>.
4. Arnsten, A.F.T., and Rubia, K. (2012). Neurobiological circuits regulating attention, cognitive control, motivation, and emotion: disruptions in neurodevelopmental psychiatric disorders. *J. Am. Acad. Child Adolesc. Psychiatry* *51*, 356–367. <https://doi.org/10.1016/j.jaac.2012.01.008>.
5. de Kloet, S.F., Bruinsma, B., Terra, H., Heistek, T.S., Passchier, E.M.J., van den Berg, A.R., Luchicchi, A., Min, R., Pattij, T., and Mansvelter, H.D. (2021). Bi-directional regulation of cognitive control by distinct prefrontal cortical output neurons to thalamus and striatum. *Nat. Commun.* *12*, 1994. <https://doi.org/10.1038/s41467-021-22260-7>.
6. Leisman, G., Braun-Benjamin, O., and Melillo, R. (2014). Cognitive-motor interactions of the basal ganglia in development. *Front. Syst. Neurosci.* *8*, 16. <https://doi.org/10.3389/fnsys.2014.00016>.
7. Pulvermüller, F. (2018). Neural reuse of action perception circuits for language, concepts and communication. *Prog. Neurobiol.* *160*, 1–44. <https://doi.org/10.1016/j.pneurobio.2017.07.001>.
8. Taghia, J., Cai, W., Ryali, S., Kochalka, J., Nicholas, J., Chen, T., and Menon, V. (2018). Uncovering hidden brain state dynamics that regulate performance and decision-making during cognition. *Nat. Commun.* *9*, 2505. <https://doi.org/10.1038/s41467-018-04723-6>.
9. Taylor, S.F., and Liberzon, I. (2007). Neural correlates of emotion regulation in psychopathology. *Trends Cognit. Sci.* *11*, 413–418. <https://doi.org/10.1016/j.tics.2007.08.006>.
10. Xu, S., Jiang, M., Liu, X., Sun, Y., Yang, L., Yang, Q., and Bai, Z. (2021). Neural Circuits for Social Interactions: From Microcircuits to Input-Output Circuits. *Front. Neural Circ.* *15*, 768294. <https://doi.org/10.3389/fncir.2021.768294>.
11. King, A.N., Barber, A.F., Smith, A.E., Dreyer, A.P., Sitarman, D., Nitabach, M.N., Cavanaugh, D.J., and Sehgal, A. (2017). A Peptidergic Circuit Links the Circadian Clock to Locomotor Activity. *Curr. Biol.* *27*, 1915–1927.e5. <https://doi.org/10.1016/j.cub.2017.05.089>.
12. Kramer, A., Yang, F.C., Snodgrass, P., Li, X., Scammell, T.E., Davis, F.C., and Weitz, C.J. (2001). Regulation of daily locomotor activity and sleep by hypothalamic EGF receptor

- signaling. *Science* 294, 2511–2515. <https://doi.org/10.1126/science.1067716>.
13. Ashhad, S., Kam, K., Del Negro, C.A., and Feldman, J.L. (2022). Breathing Rhythm and Pattern and Their Influence on Emotion. *Annu. Rev. Neurosci.* 45, 223–247. <https://doi.org/10.1146/annurev-neuro-090121-014424>.
 14. Burke, M.V., and Small, D.M. (2016). Effects of the modern food environment on striatal function, cognition and regulation of ingestive behavior. *Curr. Opin. Behav. Sci.* 9, 97–105. <https://doi.org/10.1016/j.cobeha.2016.02.036>.
 15. Cavey, M., Collins, B., Bertet, C., and Blau, J. (2016). Circadian rhythms in neuronal activity propagate through output circuits. *Nat. Neurosci.* 19, 587–595. <https://doi.org/10.1038/nn.4263>.
 16. Dinges, D.F., Pack, F., Williams, K., Gillen, K.A., Powell, J.W., Ott, G.E., Aptowicz, C., and Pack, A.I. (1997). Cumulative sleepiness, mood disturbance, and psychomotor vigilance performance decrements during a week of sleep restricted to 4–5 hours per night. *Sleep* 20, 267–277.
 17. Lieberman, H.R., Bathalon, G.P., Falco, C.M., Kramer, F.M., Morgan, C.A., 3rd, and Niro, P. (2005). Severe decrements in cognition function and mood induced by sleep loss, heat, dehydration, and undernutrition during simulated combat. *Biol. Psychiatr.* 57, 422–429. <https://doi.org/10.1016/j.biopsych.2004.11.014>.
 18. Rieger, P. (1970). Distribution of motor activity in the human circadian period. *Int. Z. Angew. Physiol.* 28, 332–343.
 19. Scott, J.P.R., McNaughton, L.R., and Polman, R.C.J. (2006). Effects of sleep deprivation and exercise on cognitive, motor performance and mood. *Physiol. Behav.* 87, 396–408. <https://doi.org/10.1016/j.physbeh.2005.11.009>.
 20. Snider, K.H., Sullivan, K.A., and Obrietan, K. (2018). Circadian Regulation of Hippocampal-dependent Memory: Circuits, Synapses, and Molecular Mechanisms. *Neural Plast.* 2018, 7292540. <https://doi.org/10.1155/2018/7292540>.
 21. Challet, E. (2019). The circadian regulation of food intake. *Nat. Rev. Endocrinol.* 15, 393–405. <https://doi.org/10.1038/s41574-019-0210-x>.
 22. Moore, R.Y., and Eichler, V.B. (1972). Loss of a circadian adrenal corticosterone rhythm following suprachiasmatic lesions in the rat. *Brain Res.* 42, 201–206. [https://doi.org/10.1016/0006-8993\(72\)90054-6](https://doi.org/10.1016/0006-8993(72)90054-6).
 23. Stephan, F.K., and Zucker, I. (1972). Circadian rhythms in drinking behavior and locomotor activity of rats are eliminated by hypothalamic lesions. *Proc. Natl. Acad. Sci. USA* 69, 1583–1586. <https://doi.org/10.1073/pnas.69.6.1583>.
 24. Evans, J.A., Suen, T.C., Callif, B.L., Mitchell, A.S., Castanon-Cervantes, O., Baker, K.M., Kloehn, I., Baba, K., Teubner, B.J.W., Ehlen, J.C., et al. (2015). Shell neurons of the master circadian clock coordinate the phase of tissue clocks throughout the brain and body. *BMC Biol.* 13, 43. <https://doi.org/10.1186/s12915-015-0157-x>.
 25. Hsu, C.T., and Sehgal, A. (2018). Circadian and Sleep Circuits Ring Together. *Neuron* 100, 514–516. <https://doi.org/10.1016/j.neuron.2018.10.030>.
 26. Jones, B.E. (2020). Arousal and sleep circuits. *Neuropsychopharmacology* 45, 6–20. <https://doi.org/10.1038/s41386-019-0444-2>.
 27. Wierzynski, C.M., Lubenov, E.V., Gu, M., and Siapas, A.G. (2009). State-dependent spike-timing relationships between hippocampal and prefrontal circuits during sleep. *Neuron* 61, 587–596. <https://doi.org/10.1016/j.neuron.2009.01.011>.
 28. Abe, M., Herzog, E.D., Yamazaki, S., Straume, M., Tei, H., Sakaki, Y., Menaker, M., and Block, G.D. (2002). Circadian rhythms in isolated brain regions. *J. Neurosci.* 22, 350–356.
 29. Cheng, H.Y.M., Alvarez-Saavedra, M., Dziema, H., Choi, Y.S., Li, A., and Obrietan, K. (2009). Segregation of expression of mPeriod gene homologs in neurons and glia: possible divergent roles of mPeriod1 and mPeriod2 in the brain. *Hum. Mol. Genet.* 18, 3110–3124. <https://doi.org/10.1093/hmg/ddp252>.
 30. Chun, L.E., Woodruff, E.R., Morton, S., Hinds, L.R., and Spencer, R.L. (2015). Variations in Phase and Amplitude of Rhythmic Clock Gene Expression across Prefrontal Cortex, Hippocampus, Amygdala, and Hypothalamic Paraventricular and Suprachiasmatic Nuclei of Male and Female Rats. *J. Biol. Rhythm.* 30, 417–436. <https://doi.org/10.1177/0748730415598608>.
 31. Guilding, C., and Piggins, H.D. (2007). Challenging the omnipotence of the suprachiasmatic timekeeper: are circadian oscillators present throughout the mammalian brain? *Eur. J. Neurosci.* 25, 3195–3216. <https://doi.org/10.1111/j.1460-9568.2007.05581.x>.
 32. Hiroshige, T., Honma, K., and Honma, S. (1991). SCN-independent circadian oscillators in the rat. *Brain Res. Bull.* 27, 441–445. [https://doi.org/10.1016/0361-9230\(91\)90139-b](https://doi.org/10.1016/0361-9230(91)90139-b).
 33. Jilg, A., Lesny, S., Peruzki, N., Schwegler, H., Selbach, O., Dehghani, F., and Stehle, J.H. (2010). Temporal dynamics of mouse hippocampal clock gene expression support memory processing. *Hippocampus* 20, 377–388. <https://doi.org/10.1002/hipo.20637>.
 34. Mure, L.S., Le, H.D., Benegiamo, G., Chang, M.W., Rios, L., Jillani, N., Ngotho, M., Kariuki, T., Dkhis-Benyahya, O., Cooper, H.M., et al. (2018). Diurnal transcriptome atlas of a primate across major neural and peripheral tissues. *Science* 359, eaao0318. <https://doi.org/10.1126/science.aao0318>.
 35. Zhang, R., Lahens, N.F., Ballance, H.I., Hughes, M.E., and Hogenesch, J.B. (2014). A circadian gene expression atlas in mammals: implications for biology and medicine. *Proc. Natl. Acad. Sci. USA* 111, 16219–16224. <https://doi.org/10.1073/pnas.1408886111>.
 36. Oh, S.W., Harris, J.A., Ng, L., Winslow, B., Cain, N., Mihalas, S., Wang, Q., Lau, C., Kuan, L., Henry, A.M., et al. (2014). A mesoscale connectome of the mouse brain. *Nature* 508, 207–214. <https://doi.org/10.1038/nature13186>.
 37. Agostinelli, F., Ceglia, N., Shahbaba, B., Sassone-Corsi, P., and Baldi, P. (2016). What time is it? Deep learning approaches for circadian rhythms. *Bioinformatics* 32, 3051. <https://doi.org/10.1093/bioinformatics/btw504>.
 38. Agostinelli, F., Ceglia, N., Shahbaba, B., Sassone-Corsi, P., and Baldi, P. (2016). What time is it? Deep learning approaches for circadian rhythms. *Bioinformatics* 32, i8–17. <https://doi.org/10.1093/bioinformatics/btw243>.
 39. Ceglia, N., Liu, Y., Chen, S., Agostinelli, F., Eckel-Mahan, K., Sassone-Corsi, P., and Baldi, P. (2018). CircadiOmics: circadian omic web portal. *Nucleic Acids Res.* 46, W157–W162. <https://doi.org/10.1093/nar/gky441>.
 40. Mei, W., Jiang, Z., Chen, Y., Chen, L., Sancar, A., and Jiang, Y. (2021). Genome-wide circadian rhythm detection methods: systematic evaluations and practical guidelines. *Briefings Bioinf.* 22, bbaa135. <https://doi.org/10.1093/bib/bbaa135>.
 41. Samad, M., Agostinelli, F., and Baldi, P. (2022). Bioinformatics and Systems Biology of Circadian Rhythms: BIO_CYCLE and CircadiOmics. *Methods Mol. Biol.* 2482, 81–94. https://doi.org/10.1007/978-1-0716-2249-0_5.
 42. Samad, M., Agostinelli, F., Sato, T., Shimaji, K., and Baldi, P. (2022). CircadiOmics: circadian omic web portal. *Nucleic Acids Res.* 50, W183–W190. <https://doi.org/10.1093/nar/gkac419>.
 43. Grillner, S., Robertson, B., and Stephenson-Jones, M. (2013). The evolutionary origin of the vertebrate basal ganglia and its role in action selection. *J. Physiol.* 591, 5425–5431. <https://doi.org/10.1113/jphysiol.2012.246660>.
 44. Stephenson-Jones, M., Ericsson, J., Robertson, B., and Grillner, S. (2012). Evolution of the basal ganglia: dual-output pathways conserved throughout vertebrate phylogeny. *J. Comp. Neurol.* 520, 2957–2973. <https://doi.org/10.1002/cne.23087>.
 45. Stephenson-Jones, M., Samuelsson, E., Ericsson, J., Robertson, B., and Grillner, S. (2011). Evolutionary conservation of the basal ganglia as a common vertebrate mechanism for action selection. *Curr. Biol.* 21, 1081–1091. <https://doi.org/10.1016/j.cub.2011.05.001>.
 46. Myers, M.G., Jr., and Olson, D.P. (2012). Central nervous system control of metabolism. *Nature* 491, 357–363. <https://doi.org/10.1038/nature11705>.
 47. Besing, R.C., Rogers, C.O., Paul, J.R., Hablitz, L.M., Johnson, R.L., McMahon, L.L., and Gamble, K.L. (2017). GSK3 activity regulates rhythms in hippocampal clock gene expression and synaptic plasticity. *Hippocampus* 27, 890–898. <https://doi.org/10.1002/hipo.22739>.
 48. Chaudhury, D., and Colwell, C.S. (2002). Circadian modulation of learning and memory in fear-conditioned mice. *Behav. Brain Res.* 133, 95–108. [https://doi.org/10.1016/s0166-4328\(01\)00471-5](https://doi.org/10.1016/s0166-4328(01)00471-5).
 49. Chaudhury, D., Wang, L.M., and Colwell, C.S. (2005). Circadian regulation of hippocampal long-term potentiation. *J. Biol. Rhythm.* 20, 225–236. <https://doi.org/10.1177/0748730405276352>.
 50. Nakatsuka, H., and Natsume, K. (2014). Circadian rhythm modulates long-term potentiation induced at CA1 in rat hippocampal slices. *Neurosci. Res.* 80, 1–9. <https://doi.org/10.1016/j.neures.2013.12.007>.
 51. Valnegri, P., Khelifaoui, M., Dorseuil, O., Bassani, S., Lagneaux, C., Gianfelice, A., Benfante, R., Chelly, J., Billuart, P., Sala, C., et al. (2011). A circadian clock in hippocampus is regulated by interaction between oligophrenin-1 and Rev-erbalpha. *Nat. Neurosci.* 14, 1293–1301. <https://doi.org/10.1038/nn.2911>.
 52. Wardlaw, S.M., Phan, T.X., Saraf, A., Chen, X., and Storm, D.R. (2014). Genetic disruption of the core circadian clock impairs hippocampus-dependent memory. *Learn. Mem.* 21, 417–423. <https://doi.org/10.1101/lm.035451.114>.

53. Ketchesin, K.D., Becker-Krail, D., and McClung, C.A. (2020). Mood-related central and peripheral clocks. *Eur. J. Neurosci.* *51*, 326–345. <https://doi.org/10.1111/ejn.14253>.
54. Qiu, M.H., Vetrivelan, R., Fuller, P.M., and Lu, J. (2010). Basal ganglia control of sleep-wake behavior and cortical activation. *Eur. J. Neurosci.* *31*, 499–507. <https://doi.org/10.1111/j.1460-9568.2009.07062.x>.
55. Qiu, M.H., Yao, Q.L., Vetrivelan, R., Chen, M.C., and Lu, J. (2016). Nigrostriatal Dopamine Acting on Globus Pallidus Regulates Sleep. *Cerebr. Cortex* *26*, 1430–1439. <https://doi.org/10.1093/cercor/bhu241>.
56. Covell, T., and Siddiqui, W. (2022). Korsakoff Syndrome. In *StatPearls*.
57. Kril, J.J., and Harper, C.G. (2012). Neuroanatomy and neuropathology associated with Korsakoff's syndrome. *Neuropsychol. Rev.* *22*, 72–80. <https://doi.org/10.1007/s11065-012-9195-0>.
58. Chen, S., Yang, J., Zhang, Y., Duan, C., Liu, Q., Huang, Z., Xu, Y., Zhou, L., and Xu, G. (2018). Ubiquitin-conjugating enzyme UBE2O regulates cellular clock function by promoting the degradation of the transcription factor BMAL1. *J. Biol. Chem.* *293*, 11296–11309. <https://doi.org/10.1074/jbc.RA117.001432>.
59. Fourriere, L., Jimenez, A.J., Perez, F., and Boncompain, G. (2020). The role of microtubules in secretory protein transport. *J. Cell Sci.* *133*, jcs237016. <https://doi.org/10.1242/jcs.237016>.
60. Hegazi, S., Cheng, A.H., Krupp, J.J., Tasaki, T., Liu, J., Szulc, D.A., Ling, H.H., Rios Garcia, J., Seecharan, S., Basiri, T., et al. (2022). UBR4/POE facilitates secretory trafficking to maintain circadian clock synchrony. *Nat. Commun.* *13*, 1594. <https://doi.org/10.1038/s41467-022-29244-1>.
61. Lecker, S.H., Goldberg, A.L., and Mitch, W.E. (2006). Protein degradation by the ubiquitin-proteasome pathway in normal and disease states. *J. Am. Soc. Nephrol.* *17*, 1807–1819. <https://doi.org/10.1681/ASN.2006010083>.
62. Lee, J., Lim, C., Han, T.H., Andreani, T., Moye, M., Curran, J., Johnson, E., Kath, W.L., Diekman, C.O., Lear, B.C., et al. (2021). The E3 ubiquitin ligase adaptor Tango10 links the core circadian clock to neuropeptide and behavioral rhythms. *Proc. Natl. Acad. Sci. USA* *118*. e2110767118. <https://doi.org/10.1073/pnas.2110767118>.
63. Mekbib, T., Suen, T.C., Rollins-Hairston, A., Smith, K., Armstrong, A., Gray, C., Owino, S., Baba, K., Baggs, J.E., Ehlen, J.C., et al. (2022). The ubiquitin ligase SIAH2 is a female-specific regulator of circadian rhythms and metabolism. *PLoS Genet.* *18*, e1010305. <https://doi.org/10.1371/journal.pgen.1010305>.
64. Mendoza-Viveros, L., Bouchard-Cannon, P., Hegazi, S., Cheng, A.H., Pastore, S., and Cheng, H.Y.M. (2017). Molecular modulators of the circadian clock: lessons from flies and mice. *Cell. Mol. Life Sci.* *74*, 1035–1059. <https://doi.org/10.1007/s00018-016-2378-8>.
65. Shi, S.Q., Mahoney, C.E., Houdek, P., Zhao, W., Anderson, M.P., Zhuo, X., Beaudet, A., Sumova, A., Scammell, T.E., and Johnson, C.H. (2022). Circadian Rhythms and Sleep Are Dependent Upon Expression Levels of Key Ubiquitin Ligase Ube3a. *Front. Behav. Neurosci.* *16*, 837523. <https://doi.org/10.3389/fnbeh.2022.837523>.
66. Hasegawa, S., Fukushima, H., Hosoda, H., Serita, T., Ishikawa, R., Rokukawa, T., Kawahara-Miki, R., Zhang, Y., Ohta, M., Okada, S., et al. (2019). Hippocampal clock regulates memory retrieval via Dopamine and PKA-induced GluA1 phosphorylation. *Nat. Commun.* *10*, 5766. <https://doi.org/10.1038/s41467-019-13554-y>.
67. Huang, S., Choi, M.H., Huang, H., Wang, X., Chang, Y.C., and Kim, J.Y. (2020). Demyelination Regulates the Circadian Transcription Factor BMAL1 to Signal Adult Neural Stem Cells to Initiate Oligodendrogenesis. *Cell Rep.* *33*, 108394. <https://doi.org/10.1016/j.celrep.2020.108394>.
68. Toda, T., Parylak, S.L., Linker, S.B., and Gage, F.H. (2019). The role of adult hippocampal neurogenesis in brain health and disease. *Mol. Psychiatr.* *24*, 67–87. <https://doi.org/10.1038/s41380-018-0036-2>.
69. Baker, P.M., Rao, Y., Rivera, Z.M.G., Garcia, E.M., and Mizumori, S.J.Y. (2019). Selective Functional Interaction Between the Lateral Habenula and Hippocampus During Different Tests of Response Flexibility. *Front. Mol. Neurosci.* *12*, 245. <https://doi.org/10.3389/fnmol.2019.00245>.
70. Halvorson, I., Gregor, L., and Thornhill, J.A. (1990). Brown adipose tissue thermogenesis is activated by electrical and chemical (L-glutamate) stimulation of the ventromedial hypothalamic nucleus in cold-acclimated rats. *Brain Res.* *522*, 76–82. [https://doi.org/10.1016/0006-8993\(90\)91579-6](https://doi.org/10.1016/0006-8993(90)91579-6).
71. Orozco-Solis, R., Aguilar-Arnal, L., Murakami, M., Peruquetti, R., Ramadori, G., Coppari, R., and Sassone-Corsi, P. (2016). The Circadian Clock in the Ventromedial Hypothalamus Controls Cyclic Energy Expenditure. *Cell Metabol.* *23*, 467–478. <https://doi.org/10.1016/j.cmet.2016.02.003>.
72. Nakamura, K., and Morrison, S.F. (2011). Central efferent pathways for cold-defensive and febrile shivering. *J. Physiol.* *589*, 3641–3658. <https://doi.org/10.1113/jphysiol.2011.210047>.
73. Refinetti, R. (2020). Circadian rhythmicity of body temperature and metabolism. *Temperature (Austin)* *7*, 321–362. <https://doi.org/10.1080/23328940.2020.1743605>.
74. Caba, M., Meza, E., Escobar, C., Jiménez, A., Caba-Flores, M.D., Moreno-Cortés, M.L., and Melo, A.I. (2021). Oxytocinergic cells of the posterior hypothalamic paraventricular nucleus participate in the food entrained clock. *Sci. Rep.* *11*, 19957. <https://doi.org/10.1038/s41598-021-99266-0>.
75. Faber, C.L., Deem, J.D., Phan, B.A., Doan, T.P., Ogomoto, K., Mirzadeh, Z., Schwartz, M.W., and Morton, G.J. (2021). Leptin receptor neurons in the dorsomedial hypothalamus regulate diurnal patterns of feeding, locomotion, and metabolism. *Elife* *10*, e63671. <https://doi.org/10.7554/eLife.63671>.
76. Gooley, J.J., Schomer, A., and Saper, C.B. (2006). The dorsomedial hypothalamic nucleus is critical for the expression of food-entrainable circadian rhythms. *Nat. Neurosci.* *9*, 398–407. <https://doi.org/10.1038/nn1651>.
77. Tran, L.T., Park, S., Kim, S.K., Lee, J.S., Kim, K.W., and Kwon, O. (2022). Hypothalamic control of energy expenditure and thermogenesis. *Exp. Mol. Med.* *54*, 358–369. <https://doi.org/10.1038/s12276-022-00741-z>.
78. Wiater, M.F., Mukherjee, S., Li, A.J., Dinh, T.T., Rooney, E.M., Simasko, S.M., and Ritter, S. (2011). Circadian integration of sleep-wake and feeding requires NPY receptor-expressing neurons in the mediobasal hypothalamus. *Am. J. Physiol. Regul. Integr. Comp. Physiol.* *301*, R1569–R1583. <https://doi.org/10.1152/ajpregu.00168.2011>.
79. Xu, B., and Xie, X. (2016). Neurotrophic factor control of satiety and body weight. *Nat. Rev. Neurosci.* *17*, 282–292. <https://doi.org/10.1038/nrn.2016.24>.
80. Acosta-Galvan, G., Yi, C.X., van der Vliet, J., Jhamandas, J.H., Panula, P., Angeles-Castellanos, M., Del Carmen Basualdo, M., Escobar, C., and Buijs, R.M. (2011). Interaction between hypothalamic dorsomedial nucleus and the suprachiasmatic nucleus determines intensity of food anticipatory behavior. *Proc. Natl. Acad. Sci. USA* *108*, 5813–5818. <https://doi.org/10.1073/pnas.1015551108>.
81. Chou, T.C., Bjorkum, A.A., Gaus, S.E., Lu, J., Scammell, T.E., and Saper, C.B. (2002). Afferents to the ventrolateral preoptic nucleus. *J. Neurosci.* *22*, 977–990.
82. Santoso, P., Nakata, M., Ueta, Y., and Yada, T. (2018). Suprachiasmatic vasopressin to paraventricular oxytocin neurocircuit in the hypothalamus relays light reception to inhibit feeding behavior. *Am. J. Physiol. Endocrinol. Metab.* *315*, E478–E488. <https://doi.org/10.1152/ajpendo.00338.2016>.
83. Lu, J., Zhang, Y.H., Chou, T.C., Gaus, S.E., Elmquist, J.K., Shiromani, P., and Saper, C.B. (2001). Contrasting effects of ibotenate lesions of the paraventricular nucleus and subparaventricular zone on sleep-wake cycle and temperature regulation. *J. Neurosci.* *21*, 4864–4874.
84. Saper, C.B., Scammell, T.E., and Lu, J. (2005). Hypothalamic regulation of sleep and circadian rhythms. *Nature* *437*, 1257–1263. <https://doi.org/10.1038/nature04284>.
85. Chevalier, G., and Deniau, J.M. (1990). Disinhibition as a basic process in the expression of striatal functions. *Trends Neurosci.* *13*, 277–280. [https://doi.org/10.1016/0166-2236\(90\)90109-n](https://doi.org/10.1016/0166-2236(90)90109-n).
86. Gerfen, C.R., and Young, W.S., 3rd (1988). Distribution of striatonigral and striatopallidal peptidergic neurons in both patch and matrix compartments: an *in situ* hybridization histochemistry and fluorescent retrograde tracing study. *Brain Res.* *460*, 161–167. [https://doi.org/10.1016/0006-8993\(88\)91217-6](https://doi.org/10.1016/0006-8993(88)91217-6).
87. Andriillon, T., and Kouider, S. (2020). The vigilant sleeper: neural mechanisms of sensory (de)coupling during sleep. *Curr. Opin. Physiol.* *15*, 47–59. <https://doi.org/10.1016/j.cophys.2019.12.002>.
88. Patel, V.R., Eckel-Mahan, K., Sassone-Corsi, P., and Baldi, P. (2012). CircadiOmics: integrating circadian genomics, transcriptomics, proteomics and metabolomics. *Nat. Methods* *9*, 772–773. <https://doi.org/10.1038/nmeth.2111>.
89. Hagberg, A., Swart, P., and Chult, D.S. (2008). Exploring Network Structure, Dynamics, and Function Using NetworkX.
90. Sievert, C. (2020). Interactive Web-Based Data Visualization with R, Plotly, and Shiny.
91. Muller, B., Richards, A.J., Jin, B., and Lu, X. (2009). GOGrapher: A Python library for GO graph representation and analysis. *BMC Res. Notes* *2*, 122. <https://doi.org/10.1186/1756-0500-2-122>.
92. Pauli Virtanen, R.G., Oliphant, T.E., Haberland, M., Reddy, T., Cournapeau, D., Burovski, E., Peterson, P., Warren, W., Bright, J., Stéfan, J., et al. (2020). SciPy. <https://doi.org/10.1038/s41592-020-0772-5>.
93. Bates, D.W., Mächler, M., Bolker, B., and Walker, S. (2015). Fitting Linear Mixed-Effects

- Models Using lme4. *BMJ Qual. Saf.* 24, 1–3. <https://doi.org/10.18637/jss.v067.i01>.
94. Seabold, S., and Perktold, J. (2010). *Statsmodels: Econometric and Statistical Modeling with python*.
95. de Manuel, M., Kuhlwilm, M., Frandsen, P., Sousa, V.C., Desai, T., Prado-Martinez, J., Hernandez-Rodriguez, J., Dupanloup, I., Lao, O., Hallast, P., et al. (2016). Chimpanzee genomic diversity reveals ancient admixture with bonobos. *Science* 354, 477–481. <https://doi.org/10.1126/science.aag2602>.
96. Someswara Rao, C., and Viswanadha Raju, S. (2016). Similarity analysis between chromosomes of *Homo sapiens* and monkeys with correlation coefficient, rank correlation coefficient and cosine similarity measures. *Genom. Data* 7, 202–209. <https://doi.org/10.1016/j.gdata.2016.01.001>.
97. Kuhlwilm, M., Gronau, I., Hubisz, M.J., de Filippo, C., Prado-Martinez, J., Kircher, M., Fu, Q., Burbano, H.A., Lalueza-Fox, C., de la Rasilla, M., et al. (2016). Ancient gene flow from early modern humans into Eastern Neanderthals. *Nature* 530, 429–433. <https://doi.org/10.1038/nature16544>.

STAR★METHODS

KEY RESOURCES TABLE

REAGENT or RESOURCE	SOURCE	IDENTIFIER
Deposited data		
Transcriptome of baboon brain (22 regions)	(Mure et al. ³⁴)	GSE98965
Allen Mouse Brain Connectivity Atlas	(Oh et al. ³⁶)	https://doi.org/10.1038/nature13186
Chimpanzee gene database	PANTHER 17.0	https://doi.org/10.5281/zenodo.7942786
Software and algorithms		
BIO_CYCLE	CircadiOmics	https://circadiomics.igb.uci.edu/
NetworkX	(Hagberg, ⁸⁹)	https://pypi.org/project/networkx/
Plotly	(Sievert, ⁹⁰)	https://github.com/plotly/plotly.py
GOGrapher	(Muller et al. ⁹¹)	https://github.com/fjukstad/gographer
SciPy	(Virtanen et al. ⁹²)	https://scipy.org/
lme4	(Bates et al. ⁹³)	https://github.com/lme4/lme4/

RESOURCE AVAILABILITY

Lead contact

Further information and requests for resources and reagents should be directed to and will be fulfilled by the lead contact, Amal Alachkar (aalachka@uci.edu).

Materials availability

This study did not generate new unique reagents.

Data and code availability

- DATA
- This paper analyzes existing, publicly available data. These accession numbers for the datasets are listed in the [key resources table](#).
- Transcriptomic datasets of baboon brain are publicly available on the CircadiOmics web portal at: <http://circadiomics.igb.uci.edu>.
- Data from the Allen Mouse Brain Connectivity Atlas are publicly available as of the date of publication.
- Transcript data of chimpanzee was accessed through the PANTHER platform and publicly available as of the date of publication.
- CODE: All original code is available at <https://github.com/pderdeyn/neural-cyclic-gene-networks>.
- Any additional information required to reanalyze the data reported in this paper is available from the [lead contact](#) upon request.

METHOD DETAILS

Transcriptomic data

Transcriptomic time series in 22 brain regions in baboon were retrieved from the publicly available database.³⁴ The original study consisted of twelve male baboons, aged between 5 to 6 years and weighing between 7 to 11 kilograms. A total of 284 brain sections were collected, amounting to 22 to 25 per animal. Samples were collected from one animal every 2 hours over a 24-hour period. To ensure the validity of the gene expression data, only genes with an average FPKM value greater than 0.1 across the 12 time points were deemed as expressed.³⁴ All tissues were immediately frozen on dry ice and stored at -80°C, preserving the integrity of RNA and ensuring high-quality sequencing data.³⁴ Brain regions included: amygdala (AMY), arcuate nucleus (ARC), cerebellum (CER), dorsomedial hypothalamus (DMH), habenula (HAB), hippocampus (HIP), prefrontal cortex (PRC), putamen (PUT), lateral globus pallidus (LGP), lateral hypothalamus (LH), mammillary body (MMB), medial globus pallidus (MGP), olfactory bulb (OLB), paraventricular nucleus (PVN), preoptic area (PRA), pons (PON), substantia nigra (SUN), suprachiasmatic nucleus (SCN), supraoptic nucleus (SON), thalamus (THA), ventromedial hypothalamus (VMH), and visual cortex (VIC).

Circadian analysis

The transcriptomic time series were extracted and analyzed through CircadiOmics,^{39,42,88} the largest repository and web portal for circadian -omic time series datasets. BIO_CYCLE, a deep-learning-based software developed to analyze periodicity in -omic time series, was used to identify statistically significant circadian transcripts and to provide the corresponding amplitudes and phases.³⁷ BIO_CYCLE

is trained and calibrated using both synthetic and real-world biological time series datasets containing labels for periodic and aperiodic signals. It uses a classification deep neural network (DNN) to discriminate periodic from aperiodic signals and a regression DNN to estimate the signal's period, phase, and amplitude. BIO_CYCLE computes p-values, and we used a cutoff of $p=0.05$ in order to consider a gene's transcript as being circadian. BIO_CYCLE is publicly available on the CircadiOmics web portal at: <http://circadiomics.igb.uci.edu>.

Cycling transcripts were clustered into four discrete time phases associated with four 6-hour intervals (quarter phases) depending on their expression peaks. Each phase is defined as follows: first quarter-phase (ZT0-ZT5), second quarter-phase (ZT6-ZT11), third quarter-phase (ZT12-ZT17), and fourth quarter-phase (ZT18-ZT23). The overlapping expression of rhythmic transcripts across different brain regions was determined through gene-view and region-view overlap. The distribution of circadian transcripts across functional brain circuits was examined and grouped based on regional localization of expression.

Network Construction

The structural network was constructed using data from the Allen Mouse Brain Connectivity Atlas,³⁶ as there currently is no equivalent meso-scale baboon or primate connectivity atlas. All experiments with injections in our regions of interest were included. One exception was the thalamus. Due to the vast number of experiments with injections that included the thalamus, we restricted the thalamus experiments to just those that primarily targeted it and manually removed a couple experiments that we found to have labeling that extended too far out of the region. The mapping between the baboon regions of interest in this manuscript and the mouse regions of interest used from the Allen Institute are in [Table S1 \(Table S1\)](#). Projections from source regions to the other regions of interest were normalized across experiments by dividing the projection density by the injection volume. For each pair of source regions and target regions, the normalized projection density was averaged across all experiments to produce a connectivity matrix. These values were then all log normalized to produce a better distribution to use as edge weights in a network. Network analysis was completed in Python using NetworkX to represent the networks.⁸⁹ Plotly was used to create network visualizations.⁹⁰ Community detection was performed using the Louvain algorithm as implemented in scikit-network with a resolution parameter of 1.⁹¹ The code used for our analysis can be found at the following link: (<https://github.com/pderdeyn/neural-cyclic-gene-networks>).

Network statistical analysis

The numbers of cyclic genes per node were compared across communities using a one-way ANOVA and then individual t-tests, both as implemented in scipy.⁹² A mixed effects model was also built to test the effect of community membership on number of cyclic genes, using the lme4 library in R.⁹³ Community membership was modeled as a random effect on number of cyclic genes. Linear correlation models were fit using ordinary least squares, implemented in Python in statsmodels. p-values of the linear coefficient were reported.⁹⁴ Heteroscedasticity of data was tested using the Breusch-Pagan test in statsmodels. Linear correlation coefficient p-values were tested for bias by scrambling the data and fitting a new linear regression model 1000 times. Monotonicity of data was tested using the Spearman correlation in scipy.

Functional enrichment analysis

Pathway enrichment analysis of cycling transcripts was performed using the PANTHER platform <http://www.pantherdb.org/>. Since the baboon gene database is not available in the Panther platform, the transcripts in the chimpanzee (Pan Troglodytes) database were selected as the reference list. Both chimpanzees (Pan troglodytes) and baboons (Papio anubis) share a common ancestor with humans. This shared lineage results in a significant degree of genetic homology among these species.^{95,96} Genome sequencing of chimpanzees and bonobos revealed a high degree of identity (approximately 98.7%) with human orthologous sequences.^{95,97} Despite their differences in cognitive abilities and social behaviors, the genetic similarities between baboons and chimpanzees have allowed to utilize the extensively annotated chimpanzee gene database for analyzing baboon gene expression data.^{95,97} Data from the PANTHER pathways annotation dataset were compared using Fisher's exact test, setting log-fold enrichment value of (2) as the threshold (FDR<0.05).

Statistical analysis

For circadian rhythm insights, transcriptomic time series data was analyzed using CircadiOmics and BIO_CYCLE, with a significance cut-off at $p=0.05$. Network analysis employed one-way ANOVA and t-tests in scipy, mixed-effects models in R's lme4, and linear models in Python's statsmodels. Functional enrichment of cycling transcripts was conducted using the PANTHER platform, leveraging the chimpanzee database due to its genetic closeness to baboons, with significance determined through Fisher's exact test at an FDR<0.05.